Steel and Composite Structures, *Vol. 23, No. 5 (2017) 611-621*
DOI: https://doi.org/10.12989/scs.2017.23.5.611

Fire resistance of high strength fiber reinforced concrete filled box columns

Chao-Wei Tang*

Department of Civil Engineering & Geomatics, Cheng Shiu University, No. 840, Chengcing Rd., Niaosong District, Kaohsiung City, Taiwan R.O.C.

(*Received October 05, 2016, Revised January 09, 2017, Accepted February 13, 2017*)

Abstract. This paper presents an investigation on the fire resistance of high strength fiber reinforced concrete filled box columns (CFBCs) under combined temperature and loading. Two groups of full-size specimens were fabricated. The control group was a steel box filled with high-strength concrete (HSC), while the experimental group consisted of a steel box filled with high strength fiber concrete (HFC) and two steel boxes filled with fiber reinforced concrete. Prior to fire test, a constant compressive load (i.e., load level for fire design) was applied to the column specimens. Thermal load was then applied on the column specimens in form of ISO 834 standard fire curve in a large-scale laboratory furnace until the set experiment termination condition was reached. The test results show that filling fiber concrete can improve the fire resistance of CFBC. Moreover, the configuration of longitudinal reinforcements and transverse stirrups can significantly improve the fire resistance of CFBCs.

Keywords: fire resistance; high strength fiber concrete; concrete filled box columns

1. Introduction

Building fires can affect the loadbearing capacity of structural bearing elements, thereby causing structural damage or collapse. Thus, most building codes stipulate that the structural members of any structure or building have to satisfy appropriate fire safety requirements (ACI-318 2014, Eurocode 2 2004, Kodur 2014). Usually, fire safety measures to structural members are measured in terms of fire resistance, which is the ability of a particular structural member to fulfil its designed function for a period of time in the event of a fire (Purkiss 2007).

The structural design of steel reinforced concrete (hereafter designated as SRC) structures can effectively combine the individual features of steel structures and reinforced concrete structures (Liu *et al*. 2014). In addition, SRC structures have several practical benefits. For instance, compared with bare steel or reinforced concrete columns, the use of concrete filled box columns (CFBCs) may have as a relatively small sectional dimension, omission of formwork and thus reducing the construction cost and time (Han *et al*. 2005). Consequently, CFBCs have been widely used in high-rise buildings and plant construction throughout the world over the past few decades (Lie and Kodur 1996, Kodur *et al*. 2004, Eurocode 4 2005, Kim *et al*. 2005, Kodur 2007, Ding and Wang 2008, Espinos *et al*. 2009, Hong and Varma 2009, Song *et al*. 2010, Aslani *et al*. 2015, Qu *et al*. 2015, Khan *et al*. 2016, Ekmekyapar 2016, Mago and Hicks 2016, Tao *et al*. 2016, Wan and Zha 2016).

In recent years, the use of high-strength concrete (hereafter designated as HSC) with compressive strength higher than 40 MPa has become increasingly popular. A number of fire test results show that there are significant differences between HSC and normal-strength concrete (NSC) after being subjected to high temperature. In general, HSC exhibits slightly lower specific heat throughout the 20–800°C temperature range, as compared to NSC (Kodur and Sultan 2003). Moreover, HSC elements are susceptible to explosive spalling when subjected to rapidly rising temperatures such as in the case of a fire (Castillo and Durrani 1990, Sanjayan and Stocks 1993, Phan and Carino 1998, 2002). Consequently, the integrity and loadbearing capacity of the structure may be reduced. However, the strength degradation in HSC at elevated temperatures is not consistent and there are significant variations in strength loss, as reported by various authors (Kodur 2014).

Fiber reinforced concrete (FRC) consists of concrete and discontinuous, discrete, uniformly dispersed fibers (Somayaji 2001). Overall, FRC is much tougher and more resistant to impact, compared to plain concrete. According to the nature of the material, fiber may be classified into metal fiber, inorganic fiber and organic fiber. Metal fibers can be further divided into steel fibers and stainless steel fibers; inorganic fibers are mainly natural and artificial mineral fibers; organic fibers are mainly synthetic fibers and plant fibers. Fibers of various shapes and sizes produced from steel, plastic, glass, and natural materials are generally being used (Metha *et al*. 2006). The tensile strength, Young's modulus, ultimate elongation, and specific gravity of various kinds of fibers are shown in Table 1 (ACI Committee 544 1982). On the other hand, aspect ratio, defined as the ratio between the fiber length and diameter, is an important characterizing parameter that affects the performance of a fiber (Somayaji 2001). Addition of fibers to concrete influences its fresh and mechanical properties which significantly depend on the

*Corresponding author, Ph.D., Professor,
E-mail: tangcw@gcloud.csu.edu.tw

ISSN: 1229-9367 (Print), 1598-6233 (Online)

Table 1 Typical types and properties of fibers

Fiber type	Tensile strength (ksi)	Young's modulus (10^3 ksi)	Ultimate elongation (%)	Specific gravity
Acrylic	30–60	0.3	25–45	1.1
Asbestos	80–140	12–20	~0.6	3.2
Cotton	60–100	0.7	3–10	1.5
Glass	150–550	10	1.5–3.5	2.5
Nylon (high tenacity)	110–120	0.6	16–20	1.1
Polyester (high tenacity)	105–125	1.2	11–13	1.4
Polypropylene	~100	0.02–0.06	~10	0.95
Polyethylene	80–110	0.5	~25	0.90
Rayon (high tenacity)	60–90	1.0	10–25	1.5
Rock wool (Scandinavian)	70–110	10–17	~0.6	2.7
Steel	40–400	29	0.5–35	7.8

type and percentage of fiber (ACI Committee 544 1982, Naaman 1985). In general, the appropriate aspect ratio of the steel fibers is about 50 to 100, and the fiber content is generally 1 to 2% (volume percentage). In practice, the workability of FRC decreases with increasing aspect ratio. In particular, if the aspect ratio is greater than about 100, it is very difficult to achieve a uniform mix (Swamy and Mangat 1974).

Since the 1970s, a great number of fire, static, and dynamic tests have been carried out to explore the effects of type, shape, aspect ratio and content of the fiber on the mechanical properties of FRC and the toughness of FRC components (Krenchel 1974, Swamy and Mangat 1974, ACI Committee 544 1982, Bilodeau *et al*. 2004, Sideris *et al*. 2009, Ding *et al*. 2012, Ozawa and Morimoto 2014, Yan *et al*. 2015, Kim *et al*. 2016, Lee and Yi 2016, Xu *et al*. 2016). It was observed that the extent of explosive spalling can considerably be reduced by use of adequate amount of polypropylene (PP) fibers (Hannant 1998, Tatnall 2002, Atkinson 2004, Larbi and Polder 2007). The reason is the burning of PP fibers produces microchannels for release of vapor pressure of concrete, and thus the amount of heat absorbed is less for dehydration of chemically bound water (Bilodeau *et al*. 2004, Kodur 2014). As a result, its specific heat is reduced in the temperature range of 600–800°C (Kodur 2014). In other words, during the high temperature, PP fibers can mitigate or prevent the explosive spalling (Atkinson 2004, Poon *et al*. 2004, Sideris *et al*. 2009, Ding *et al*. 2012, Ozawa and Morimoto 2014, Yan *et al*. 2015). In addition, Ozawa et al. studied the spalling behavior of ultra-high-strength fiber-reinforced concrete (UFC) with PP, jute, and water soluble polyvinyl alcohol (WSPVA) fiber in the temperature range of 400–800°C. They inferred that adding 0.19% by volume of natural jute fibers to UFC is an effective method in the prevention of spalling-related damage (Ozawa *et al*. 2014). In view of the above, this study aims to investigate the fire resistance of high strength fiber reinforced concrete filled box columns under combined temperature and loading.

2. Experimental procedure

2.1 Experimental program

The design and planning of CFBC specimens are given in Table 2. As can be seen from Table 2, two groups of full-size specimens were cast to consider the effect of type of concrete infilling on the fire resistance of CFBCs. The control group was a steel box filled with HSC, while the experimental group consisted of a steel box filled with high strength fiber concrete (HFC) and two steel boxes filled with fiber reinforced concrete. Take into account the rheological and mechanical properties of the HFC, the fiber content used was 1% (volume fraction). The presence of fibers at this volume fraction can avoid the workability problem (balling and clumping of fibers) of composites associated with the addition of PP fibers. At the same time, it can increase the modulus of rupture and fracture toughness of the HFC. In addition to CFBC's fire test, the residual compressive strength of HSC and HFC cylinders (120 mm diameter × 240 mm height) after exposure to elevated temperatures was also carried out.

2.2 Casting of specimens

The column specimens had square cross sections, as shown in Fig. 1. All the columns were 3000 mm long. All the steel sections of the specimens were made of steel plates

Table 2 Design of CFBC specimens and summary of test information

Group type	Specimen No.	$\eta_{fi,t}$	F	R	u_s (mm)	S (mm)	F_{ys} (MPa)	E_s (GPa)	F_{yr} (MPa)	f_c' (MPa)	Slump (mm)	Slump flow (mm)
Control group	C1	0.28	-	0	-	-	414	205.9		48	270	745
Experimental group	E1	0.28	1%	0	-	-	414	205.9		44	250	540
	E2	0.28	1%	6%	60	150	414	205.9	483	44	250	540
	E3	0.28	1%	6%	60	300	414	205.9	483	44	250	540

*Notes: $\eta_{fi,t}$ = load level for fire design; F = fiber content (Volume %); R = reinforcement ratio=$A_s/(A_s+A_c)$, A_c = cross-sectional area of the concrete, A_s = cross-sectional area of the reinforcing bars; u_s = minimum axial distance of reinforcing bars; S = stirrup spacing; F_{ys} = yield strength of the steel; E_s = steel modulus of elasticity; F_{yr} = yield strength of the reinforcing bars; f_c' = compressive strength of concrete

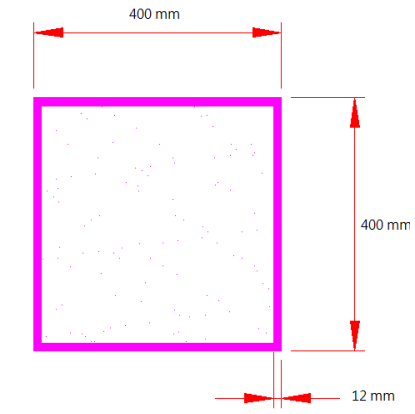

(a) Control group

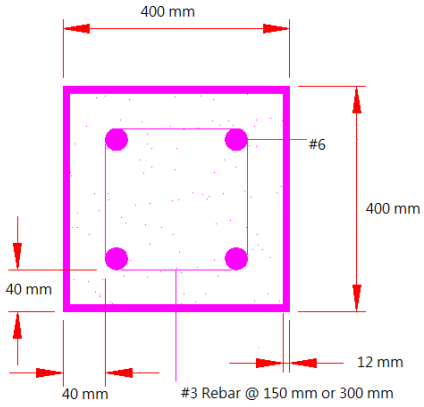

(b) Experimental group

Fig. 1 Cross section of CFBC specimens

of 12 mm thickness. These plates were joined by longitudinal full penetration welding. To achieve composite action between the concrete and steel plates, shear studs were provided for all the column specimens. In addition, no external fire-proofing was provided for the steel.

The cement used here was Type I Portland cement with a specific gravity of 3.15 and a fineness of 3400 cm^2/g. The fine aggregate was natural river sand. The coarse aggregate was crushed stone with a maximum particle size of 19 mm. The density of the polypropylene fiber used was 0.9 g/cm^3. The mix proportions for the concrete are shown in Table 3. The fiber content in the experimental group was 1% of the concrete volume. The slump flow test, V-funnel test, and passing ability using U-type test were adopted to assess the workability of the concrete. The aforementioned test results met regulatory requirements for self-compacting concrete. The average measured cylinder compressive strength (f'_c) on the testing day for different column specimens was 44–48 MPa.

Table 3 Mix proportions of concrete

Cement (kg/m^3)	Slag (kg/m^3)	Fly ash (kg/m^3)	Water (kg/m^3)	FA (kg/m^3)	CA (kg/m^3)	SP (kg/m^3)
356	76	76	178	889	780	8.14

*Notes: FA = fine aggregate, CA = coarse aggregate, SP = superplasticizer (HICON MTP A40)

Freshly mixed concrete was slowly poured in the steel box columns by use of a concrete placement bucket and a funnel, followed by controlled vibrations. Along with each mix, enough cylindrical specimens were cast for compressive strength test. All the column specimens and cylinders were covered with a wet hessian and plastic sheets overnight. Then, the cylinders were removed from the molds. Following demolding, the cylinders were immediately submerged in a water curing tank in the laboratory until the time of testing. All the column specimens were placed indoors for 91 days under indoor curing conditions. On the other hands, the compressive strength of three concrete cylinders for each mixture proportion was tested at ages of 3, 7, 14, 28, 56, and 91 days, respectively.

2.3 Test set up and procedure

Prior to the fire test, the column specimen was installed in the furnace as shown in Fig. 2; and then a constant compressive load (i.e., load level for fire design) was applied to the column specimen. The load level for fire design corresponded to 28% of the nominal compressive strength of the specimen, which is the design value of the buckling resistance of the column at room temperature. The nominal compressive strength *Pn* is defined in the Taiwan Design Code for SRC Structures (Taiwan Construction and Planning Agency 2004) as

$$P_n = \phi_{cs} P_{ns} + \phi_{crc} P_{nrc} \quad (1)$$

where P_{ns} = nominal steel compressive strength; P_{nrc} = nominal compressive strength of the reinforced concrete of

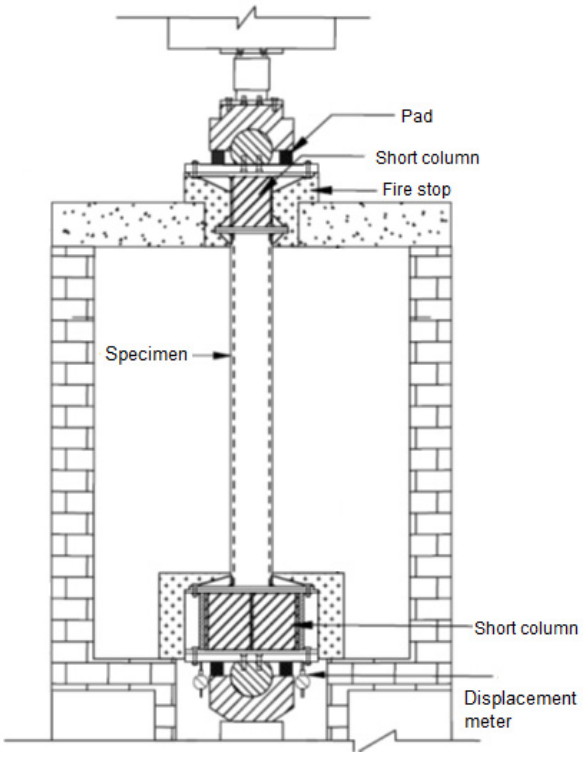

Fig. 2 Test setups for CFBC specimens

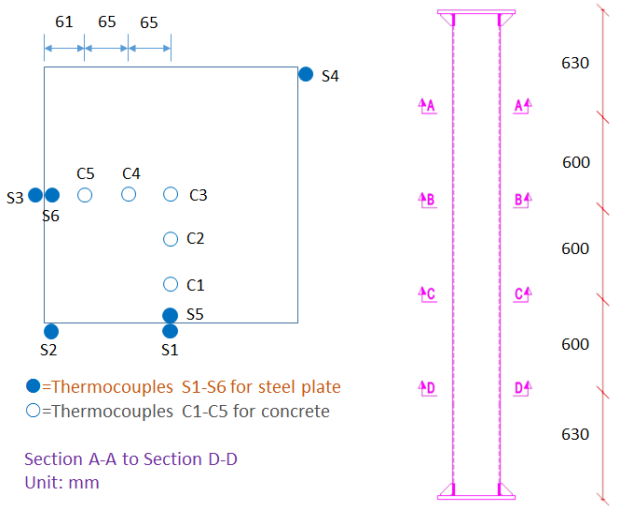

Fig. 3 Scheme and thermocouples layout of CFBC

the SRC column; ϕ_{cs} and ϕ_{crc} = resistance factors for compression.

The temperature from the specimen's surface to the inner central core was measured with type K thermocouples. Fig. 3 shows the thermocouples were placed at different depths in four sections of the column. In each section (Fig. 3), six thermocouples (i.e., S1-S6) were welded to the steel plate surface, while five thermocouples (i.e., C1-C5) were embedded in the concrete core at different depths. To measure the axial displacements of the columns, linear variable displacement transducers were used. They were placed on the top and bottom of the test columns. Thermal load was applied on the columns in form of ISO 834 standard fire curve in a large-scale laboratory furnace until the set experiment termination condition was reached. The temperature inside the furnace was controlled by 18 gas burners, and 14 thermocouples were used to monitor the furnace temperature at different locations. The current failure criterion specified in ISO 834 is adopted in this study, which is based on the amount of contraction and the rate of contraction. For the columns under consideration, these criteria correspond to a maximum contraction of 30 mm and a rate of contraction of 9 mm/min.

Besides, on the testing day for CFBC specimens, the cylindrical HSC and HFC specimens were placed in a computer-controlled electric furnace for performing a high temperature test. The specimen was heated without preload at a prescribed rate (10°C/min) until the temperature inside the furnace reached the target temperatures (i.e., 200, 400, 600 and 800°C, respectively). Once the targeted peak temperature was reached, the furnace temperature was maintained for another hour to achieve a thermal steady state (Fig. 4). The furnace was then switched off, and the cylindrical specimens were allowed to cool naturally in the furnace with the door opened. After the cylindrical specimens cooled to room temperature, the residual compressive strength test was carried out in a compression machine.

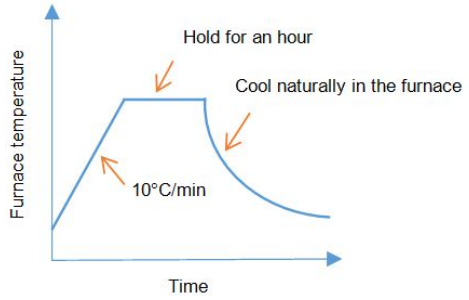

Fig. 4 Temperature versus time curve in the furnace for the cylindrical HSC and HFC specimens

3. Experimental results and discussion

3.1 Residual compressive strength of cylindrical HSC and HFC specimens

The residual compressive strength of concrete subjected to high temperatures has a close relationship with the factors such as dehydration and transformation reactions, changes in porosity and pore pressures, and the differential deformation of hardened cement paste and aggregates. Therefore, the results of different researchers on the residual compressive strength of concrete exposed to high temperatures show that there are significant differences. The effect of temperature on the residual compressive strength of HSC and HFC is shown in Fig. 5. Test results show that there was an increase of about 3-15% of the original unheated value at temperatures up to 400°C. This was similar to those reported by other researchers

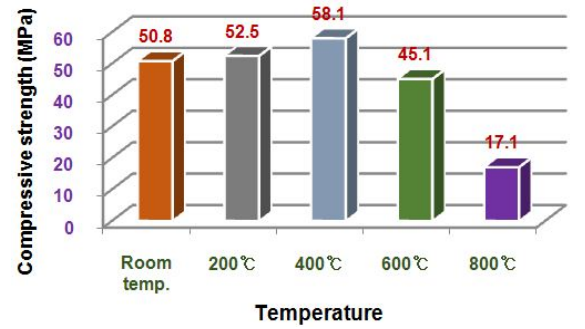

(a) HSC specimens

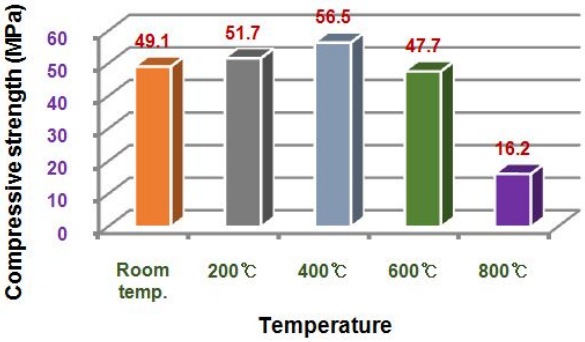

(b) HFC specimens

Fig. 5 Effect of temperature on the residual compressive strength of cylindrical specimens

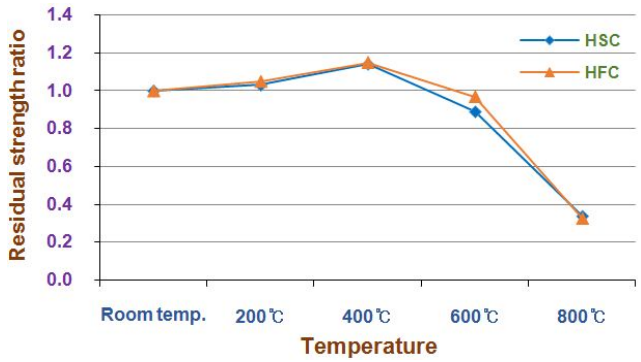

Fig. 6 Effect of temperature on the residual strength ratio of cylindrical specimens

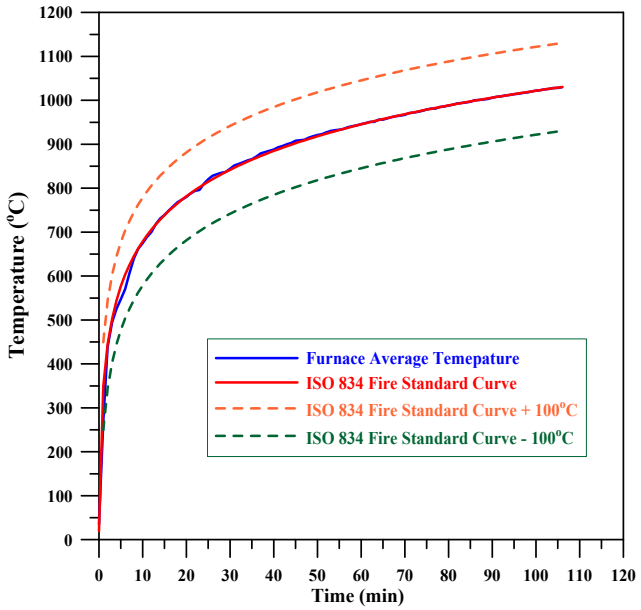

Fig. 7 Temperature versus time curves in the furnace for the 2 specimen

(Chakrabari *et al*. 1994, Janotka and Bágel 2003, Toumi *et al*. 2009, Li and Bu 2011, Hachemi *et al*. 2014, Mundhada *et al*. 2015). The residual compressive strength increased at 200°C by 3.3% and 5.2% for the HSC and HFC respectively, as compared with the room-temperature strength. With a further increase in temperature to 400°C, the HSC and HFC specimens reached a peak strength of 14–15% above room temperature strength. This is because the temperature inside the test specimen was still lower than 400 °C although the furnace temperature was maintained for one hour. In other words, the average temperature of the test specimen had not yet reached 400°C. Owing to rapid drying of the concrete, the pore water, adsorbed water and interlayer water in the specimen can be easily evaporated (Siddique and Kaur 2012). Thus, the residual compressive strength increased. However, at 600°C, the average temperature inside the concrete specimen should exceed 400°C, the compressive strength should decay, and its destruction caused by brittleness. As a result, the residual compressive strength of the HSC specimen dropped by 11.2% as compared with the room-temperature strength, while the HFC specimen only dropped by 3.0% as compared with the room-temperature strength.

In addition, Fig. 6 shows the residual compressive strength ratio (i.e., residual compressive strength to room-temperature strength) for the HSC and HFC cylindrical specimens. As shown in Fig. 6, the residual compressive strength of the HFC is superior than that of the HSC. At 200 and 400°C, the residual compressive strengths of the HFC were slightly better than those of the HSC. At a temperature of 600°C, the residual compressive strength of the HFC can still maintain 97% of the room-temperature strength, while the residual compressive strength of the HSC was only 89% of the room-temperature strength. This showed that the incorporation of polypropylene fiber can reduce the formation pore pressure of concrete at high temperature, thereby reducing the occurrence of concrete disintegration. When the temperature was raised to 800°C, the residual compressive strength of the HSC and HFC specimens was about 67% lower than that of the control at room temperature. In other words, the strength loss was very significant.

3.2 Furnace temperature versus time

Prior to the fire test, the predetermined axial compression load was applied to the column specimens. According to Eq. (1), the applied axial compressive loads were 2754 KN and 2656 KN for the control group and the experimental group respectively. Then four CFBCs were tested to failure by exposing the loaded columns to fire. During the test, the column was exposed to heating controlled in such a way that the average temperature in the furnace followed, as closely as possible, the standard time-temperature curve of ISO 834. For example, Fig. 7 shows the furnace temperature in the fire resistance tests for the E2 specimen. It can be seen that when the time was between 0 and 10 min., the furnace temperature in the fire resistance tests was a little lower than the ISO 834 fire curve. After more than ten minutes, however, the temperature followed nearly the ISO 834 fire curve and was very uniform in the fire tests.

3.3 Fire test results

Fire tests were carried out on the column specimens. As expected, it was observed that the columns expand in the initial stages and then contract leading to failure. The effect of load and thermal expansion is significant in the early stages, while the effect of creep becomes pronounced in the later stages. This result was similar to those reported by other researchers (Lie and Kodur 1996, Kodur 1999). After the column specimens reached the aforementioned failure criterion, the furnace was switched off and the cooling took place in the furnace with the door closed. The fire test results such as fire resistance, maximum axial deformation, average temperature of steel plate upon termination, average temperature of concrete upon termination, maximum temperature of steel plate upon termination, and maximum temperature of concrete upon termination are shown in Table 4. As previously stated, the temperature from the specimen's surface to the inner central core was

Table 4 Fire test results

Item	Specimen No.			
	C1	E1	E2	E3
Duration of fire test (min)	41	47	106	69
Fire resistance (min)	40	46	105	68
Maximum axial deformation (mm)*	13.6	13.9	12.7	11.7
Time required to reach maximum elongation (min)	26	27	25	24
Average temperature of steel plate upon termination (°C)	663.6	622.4	934.9	690.1
Maximum temperature of steel plate upon termination (°C)	822.1	823.5	1035.8	892.0
Average temperature of concrete upon termination (°C)	117.7	145.4	500.9	289.1
Maximum temperature of concrete upon termination (°C)	152.4	276.0	618.2	556.3

*Note: Positive values indicate expansion and negative contraction

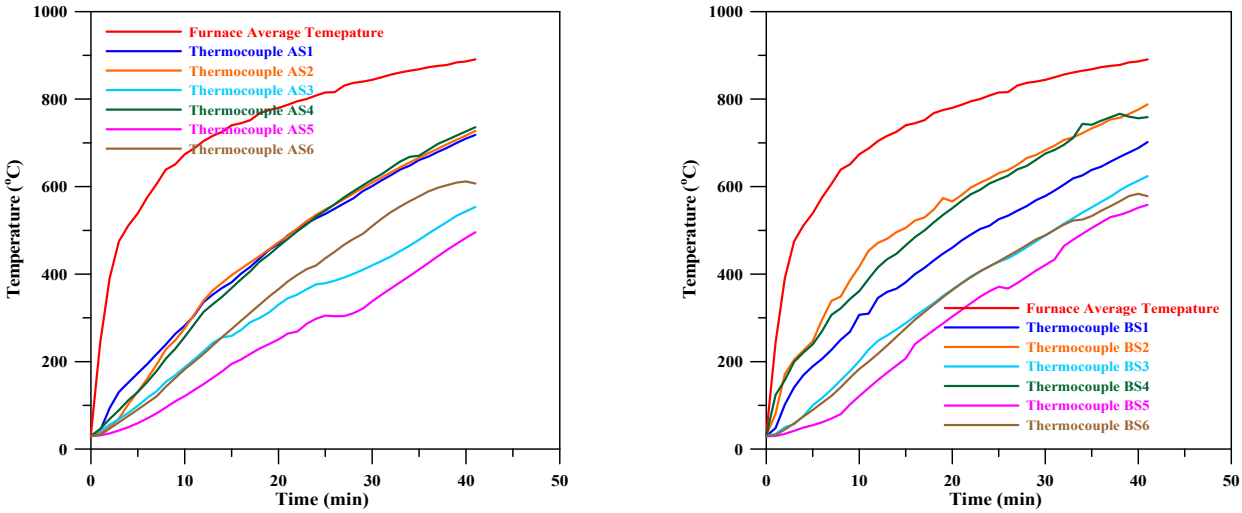

(a) Section A (b) Section B

Fig. 8 Temperature of steel plate versus time curves for the C1 specimen

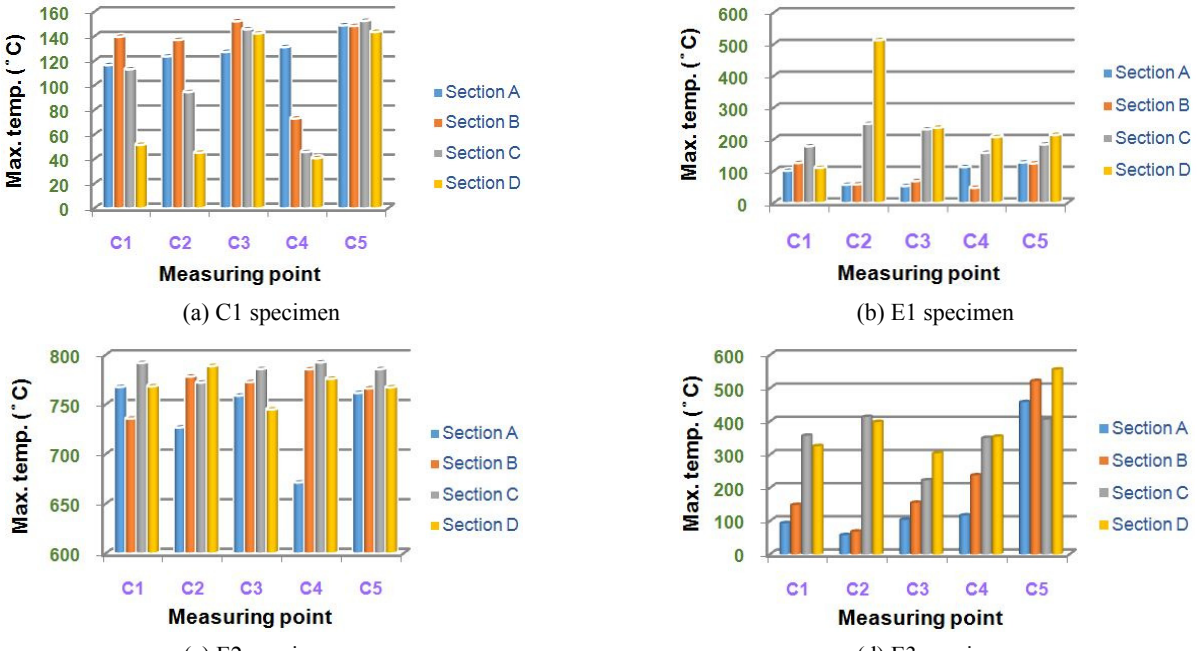

(a) C1 specimen (b) E1 specimen

(c) E2 specimen (d) E3 specimen

Fig. 9 Maximum temperature of the concrete thermocouple for CFBC specimens

Table 5 Ahpgxial deformation for column specimens

Fire duration (min.)	Axial deformation (mm)			
	C1 specimen	E1 specimen	E2 specimen	E3 specimen
5	0.9	0.8	1.1	1.2
10	4.8	4.2	4.6	4.9
15	8.5	7.9	8.2	8.1
20	11.7	11.3	11.3	11.0
25	13.5	13.6	12.7	11.6
30	10.6	12.5	9.2	7.1
35	2.9	4	5.2	3.7
40	-7	-1	3.1	1.
45	-	-9.5	1.5	-0.6
50	-	-	0.4	-2.2
55	-	-	-0.4	-4.2
60	-	-	-1.1	-7.7
65	-	-	-1.6	-12.5
70	-	-	-1.9	-
75	-	-	-2.3	-
80	-	-	-2.8	-
85	-	-	-3.3	-
90	-	-	-4.0	-
95	-	-	-4.9	-
100	-	-	-6.2	-
105	-	-	-10.3	-

*Note: Positive values indicate expansion and negative contraction

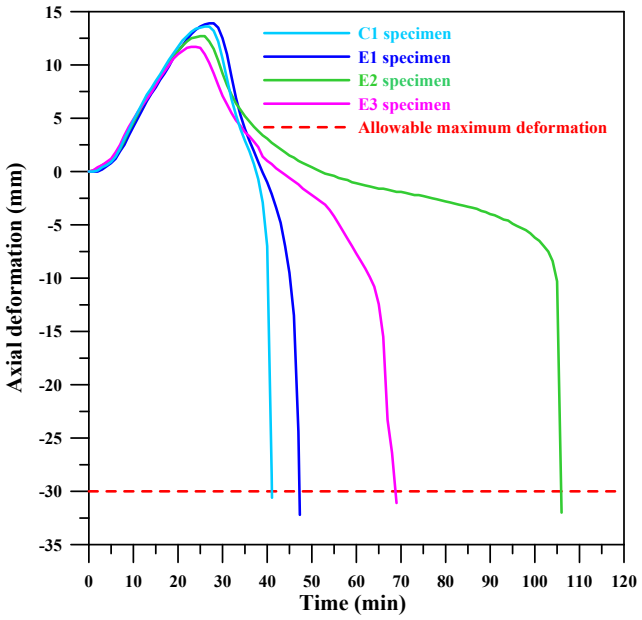

Fig. 10 Axial deformation versus time curves for CFBC specimens

measured with type K thermocouples located at different depths in four sections of the column (Fig. 3). Throughout the fire test, the temperature of the steel plates rose with the increasing temperature of the furnace. For example, Fig. 8 shows the temperature of steel plate versus time curves for the C1 specimen. As can be seen in Table 4, the maximum temperatures of steel plate upon termination were 822.1, 823.5, 1035.8 and 892.0°C for the C1, E1, E2, and E3

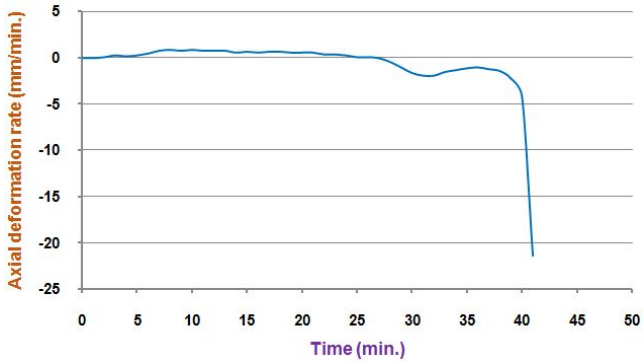

(a) C1 specimen

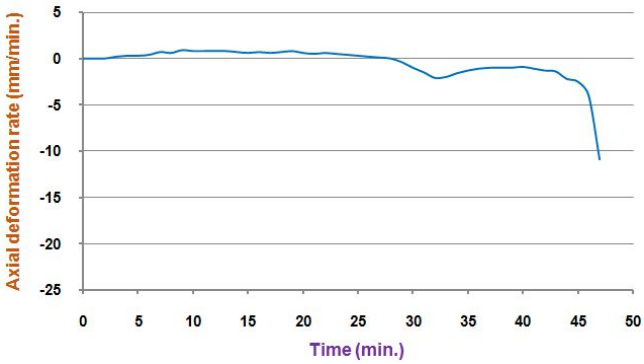

(b) E1 specimen

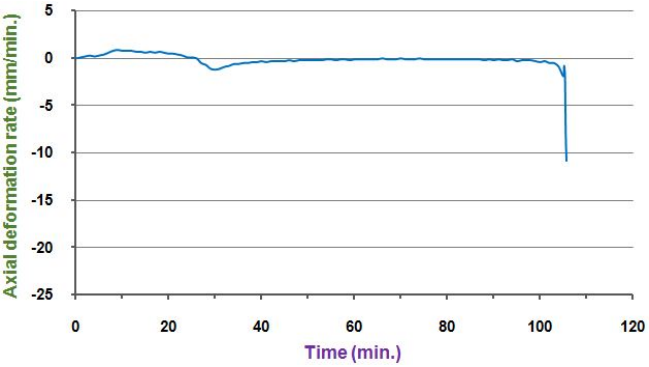

(c) E2 specimen

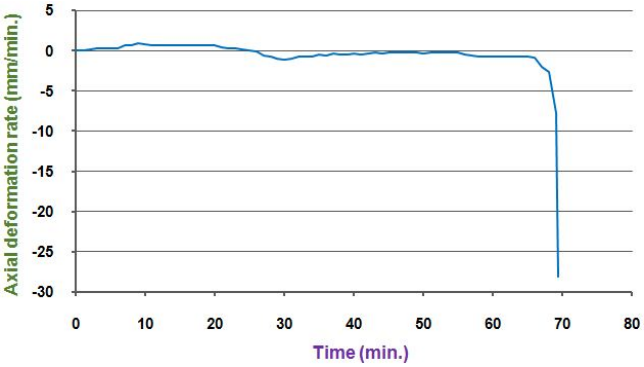

(d) E3 specimen

Fig. 11 Axial deformation rate versus time curves for the CFBC specimens

specimens, respectively.

In addition, the recorded maximum temperature at various locations within the concrete of the C1, E1, E2, and E3 specimens are shown in Fig. 9. Taking the E2 specimen as an example, it can be seen from Fig. 9(c) that the maximum temperature recorded on the C5 measuring point of the four sections was above 760°C. However, there was a significant difference in the maximum temperature of each section at other measuring points. Moreover, the highest temperature recorded on of the concrete core (i.e., C3 measuring point) during the E2 specimen fire test was about 786°C, which appeared in section C. However, the highest temperature recorded on the concrete core during the fire tests of the C1 and E1 specimens was much lower (approximately 152°C for the C1 specimen and 238°C for the E1 specimen). The reason is the E2 specimen was exposed to fire for about 60 minutes longer than the C1 and E1 specimens.

3.4 Axial deformation

Axial deformations for all the column specimens are shown in Table 5. The axial deformation of the columns was measured by LVDTs and displacement meters located outside the furnace. The deformation in these columns is caused by several major factors, such as load, thermal expansion and creep. The contraction in the column length under the applied load is attenuated by material property deterioration at elevated temperatures. Whereas the column subjected to high temperatures caused thermal expansion. In other words, the observed axial deformations of the column specimens were the result of a combination of the mechanical and thermal load.

Fig. 10 shows the axial deformation (y-axis) versus time (x-axis) curve registered during the fire test. Obviously, the columns experienced an expansion phase before being compressed to failure due to the thermal expansion

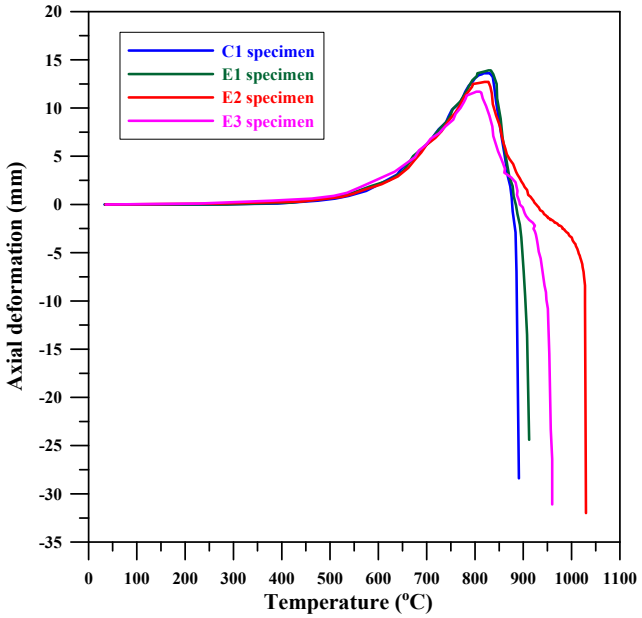

Fig. 12 Axial deformation versus temperature curves for CFBC specimens

behavior of the material. Basically, due to its higher thermal conductivity and its direct exposure to fire, the steel plate heated up more rapidly and subsequently expanded faster than the core concrete (Kodur 2007). Moreover, with the increased fire time, the specimen axial deformation increases, until the maximum elongation. At that point, contraction began immediately, as shown in Fig. 10. Taking the C1 specimen as an example, it is shown in Table 5 that during the first 20 minutes in the fire damage test, C1 specimen's axial elongation was greater than that of the E1 specimen. Moreover, Fig. 11 shows the axial deformation rate versus time curves for the C1 and E1 specimens, respectively. It can be clearly seen in Fig. 11 that C1 specimen's axial deformation rate was -21.4 mm/min when the fire duration reached 41 minutes. In other words, the compressive deformation rapidly increased at this moment. In contrast, the E1 specimen was obviously compressed until 47 minutes. Therefore, the E1 specimen filled with fiber concrete had a better fire behavior. On the other hand, Fig. 12 shows the axial deformation versus temperature for all the CFBC specimens. As can be seen in Fig. 12, the specimens began to elongate when the average temperature of the furnace reached about 390°C; the axial elongation of the specimens increased rapidly when the average temperature of the furnace was between 750–830°C; the axial compressive deformation sharply increased in a very short time when the average temperature of the furnace was between 880–890°C.

3.5 Fire resistance

Due to the experimental group filled with fiber concrete, or configured with longitudinal reinforcements and transverse stirrups, their fire resistances are quite better than that of the control group. Results from the fire tests indicate that the fire resistance of the E1 specimen was 46 minutes, as compared with 40 minutes for the C1 specimen. This result shows that filling fiber concrete can improve the fire resistance of CFBCs. In addition, the fire resistance of the E2 specimen was 105 minutes, as compared with 46 minutes for the E1 specimen. As a result, it can be concluded that the presence of rebars not only decreases the propagation of cracks and sudden loss of strength, but also contributes to the load-carrying capacity of the concrete core. This result shows that the configuration of longitudinal reinforcements and transverse stirrups can significantly improve the fire resistance of CFBCs. Moreover, under the same load level for fire design, the fire resistance of the E2 specimen with transverse stirrup spacing of 15 cm was 105 minutes, while the fire resistance of the E3 specimen with stirrup spacing of 30 cm was reduced to 68 minutes. This indicates that the stirrup spacing is closely related to the fire resistance of CFBCs.

On the other hand, after the CFBC specimens had been cooled, their failure modes were observed. Basically, there was no cracking in the welding bead of the specimens. In other words, no crack was detected in any of the specimens. Overall, the failure was either by local buckling or general instability. Fig. 13 shows the appearance of the C1, E1, and E2 specimens after the fire test. It can be clearly seen that the final failure mode was the local bulge of the column

(a) Appearance of the C1 specimen

(b) Appearance of the E1 specimen

(c) Appearance of the E2 specimen

(d) Bulge of the C1 specimen

(e) Bulge of the E1 specimen

(f) Bulge of the E2 specimen

Fig. 13 A general view of the specimens after test

steel plates. As demonstrated in Fig. 13, the local bulge of the column steel plates occurred at several locations were observed. Taking the E2 specimen as an example, it can be seen from Fig. 13(f) that a prominent bulge was observed in the web near mid-height of the column.

4. Conclusions

Based on the experimental results, the following conclusions can be drawn:

- At a temperature of 600°C, the residual compressive strength of the cylindrical HFC specimens can still maintain 97% of the room-temperature strength, while the residual compressive strength of the cylindrical HSC specimens was only 89% of the room-temperature strength. This showed that the incorporation of polypropylene fiber can reduce the formation pore pressure of concrete at high temperature, thereby reducing the occurrence of concrete disintegration.
- The CFBC specimens began to elongate when the average temperature of the furnace reached about 390°C; the axial elongation of the CFBC specimens increased rapidly when the average temperature of the furnace was between 750–830°C; while the axial compressive deformation sharply increased in a very short time when the average temperature of the furnace was between 880–890°C.
- Under the same load level for fire design, the fire resistance of the E1 specimen was 46 minutes, as compared with 40 minutes for the C1 specimen. This result shows that filling fiber concrete can improve the fire resistance of CFBCs.
- The fire resistance of the E2 specimen was 105 minutes, as compared with 46 minutes for the E1 specimen. Therefore, it can be concluded that the configuration of longitudinal reinforcements and transverse stirrups can significantly improve the fire resistance of CFBCs.
- The fire resistance of the E2 specimen with transverse stirrup spacing of 15 cm was 105 minutes, while the fire resistance of the E3 specimen with stirrup spacing of 30 cm was reduced to 68 minutes. This indicates that the stirrup spacing is closely related to the fire resistance of CFBCs.

On the other hand, according to the results of this study, some recommendations can be provided for the fire resistance of CFBCs. Overall, CFBCs possesses excellent structural behavior. The filling of concrete or reinforced concrete can enhance the stiffness of box column. Besides, it offers a practical solution for providing fire protection to hollow structural steel columns without any external protection.

Acknowledgments

The research described in this paper was supported by the Architecture and Building Research Institute (ABRI), Ministry of the Interior, Taiwan. The author expresses his gratitude and sincere appreciation to ABRI for financing this research work.

References

ACI Committee 544 (1982), "State of the art report of fiber reinforced concrete", *Concr. Int.: Des. Construct.*, **4**(5), 9-30.

ACI-318 (2014), Building code requirements for reinforced concrete and commentary; American Concrete Institute, Farmington Hills, MI, USA.

Aslani, F., Uy, B., Tao, Z. and Mashiri, F. (2015), "Predicting the axial load capacity of high-strength concrete filled steel tubular columns", *Steel Compos. Struct., Int. J.*, **19**(4), 967-993.

Atkinson, T. (2004), "Polypropylene fibers control explosive spalling in high performance concrete", *Concrete*, **38**(10), 69-

70.
Bilodeau, A., Kodur, V.K.R. and Hoff, G.C. (2004), "Optimization of the type and amount of polypropylene fibres for preventing the spalling of lightweight concrete subjected to hydrocarbon fire", *Cement Concrete Compos*., **26**(2), 163-174.
Castillo, C. and Durrani, A.J. (1990), "Effect of transient high temperature on high-strength concrete", *ACI Mater. J*., **87**(1), 47-53.
Chakrabari, S.C., Sharma, K.N. and Mittal, A. (1994), "Residual strength in concrete after exposure to elevated temperature", *Indian Concrete J*., December, 713-717.
Ding, J. and Wang, Y.C. (2008), "Realistic modelling of thermal and structural behaviour of unprotected concrete filled tubular columns in fire", *J. Constr. Steel Res*., **64**(10), 1086-1102.
Ding, Y., Azevedo, C., Aguiar, J.B. and Jalali, S. (2012), "Study on residual behaviour and flexural toughness of fibre cocktail reinforced self compacting high performance concrete after exposure to high temperature", *Constr. Build. Mater*., **26**(1), 21-31.
Ekmekyapar, T. (2016), "Experimental performance of concrete filled welded steel tube columns", *J. Constr. Steel Res*., **117**, 175-184.
Espinos, A., Hospitaler, A. and Romero, M.L. (2009), "Fire resistance of axially loaded slender concrete filled steel tubular columns", *Acta Polytechnica*, **49**(1), 39-43.
Eurocode 2 (2004), Design of concrete structures. Part 1-2: general rules—structural fire design; European Committee for Standardization, Brussels, Belgium.
Eurocode 4 (2005), Design of composite steel and concrete structures–Part 1-2: General–Structural fire design.
Hachemi, S., Ounis, A. and Chabi, S. (2014), "Evaluating residual mechanical and physical properties of concrete at elevated temperatures", *Int. J. Civil, Environ., Struct., Constr. Architect. Eng*., **8**(2), 176-181.
Han, LH., Yao, G.H. and Zhao, X.L. (2005), "Tests and calculations for hollow structural steel (HSS) stub columns filled with self-consolidating concrete (SCC)", *J. Constr. Steel Res*., **61**(9), 1241-1269.
Hannant, D.J. (1998), "Durability of polypropylene fibers in Portland cement-based composites: Eighteen years of data", *Cement Concrete Res*., **28**(12), 1809-1817.
Hong, S. and Varma, A.H. (2009), "Analytical modeling of the standard fire behavior of loaded CFT columns", *J. Constr. Steel Res*., **65**, 54-69.
Janotka, I. and Bágel, L. (2003), "Pore structures, permeabilities and compressive strengths of concrete at temperatures up to 800 °C", *ACI Mater J*, **100**(1), 87-89.
Khan, Q.S., Sheikh, M.N. and Hadi, M.N.S. (2016), "Axial compressive behaviour of circular CFFT: Experimental database and design-oriented model", *Steel Compos. Struct., Int. J*., **21**(4), 921-947.
Kim, D.K., Choi, S.M., Kim, J.H., Chung, K.S. and Park, S.H. (2005), "Experimental study on fire resistance of concrete-filled steel tube column under constant axial loads", *Steel Struct*., **5**(4), 305-313.
Kim, N.W., Lee, H.H. and Kim, C.H. (2016), "Fracture behavior of hybrid fiber reinforced concrete according to the evaluation of crack resistance and thermal", *Computers Concrete*, **18**(5), 685-696.
Kodur, V.K.R. (1999), "Performance-based fire resistance design of concrete-filled steel columns", *J. Constr. Steel Res*., **51**(1), 21-36.
Kodur, V.K.R. (2007), "Guidelines for fire resistant design of concrete-filled steel HSS columns-state-of-the-art and research needs", *Steel Struct*., **7**(3), 173-182.
Kodur, V. (2014), "Properties of concrete at elevated temperatures", *ISRN Civil Engineering Volume*, Article ID 468510.
Kodur, V.K.R. and Sultan, M.A. (2003), "Effect of temperature on thermal properties of high-strength concrete", *J. Mater. Civil Eng*., **5**(2), 101-107.
Kodur, V.K.R., Wang, T.C. and Cheng, F.P. (2004), "Predicting the fire resistance behavior of high strength concrete columns", *Cement Concrete Compos*., **26**(2), 141-153.
Krenchel, H. (1974), *Fiber Reinforced Concrete*, ACI SP-44, pp. 45-77.
Larbi, J.A. and Polder, R.B. (2007), "Effects of polypropylene fibres in concrete: Microstructure after fire testing and chloride migration", *Heron*, **52**(4), 289-306.
Lee, H.H. and Yi, S.T. (2016), "Structural performance evaluation of steel fiber reinforced concrete beams with recycled aggregates", *Comput. Concrete*, **18**(5), 741-756.
Li, X. and Bu, F. (2011), "Residual strength for concrete after exposure to high temperatures", *Innov. Comput. Info*., **232**, 382-390.
Lie, T.T. and Kodur, V.K.R. (1996), "Fire resistance of steel columns filled with bar-reinforced concrete", *ASCE J. Struct. Eng*., **122**(1), 30-36.
Liu, B., Tong, L. and Zhao, X.L. (2014), "Fatigue failure characteristics of steel reinforced concrete girders", *Procedia Mater. Sci*., **3**, 1717-1722.
Mago, N. and Hicks, S.J. (2016), "Fire behaviour of slender, highly utilized, eccentrically loaded concrete filled tubular columns", *J. Constr. Steel Res*., **119**, 123-132.
Metha, P.K. and Monteiro, P.J.M. (2006), *Concrete*; *Microstructure*, *Properties and Materials*, (3rd Edition), McGraw-Hill, New York, NY, USA.
Mundhada, A.R. and Pofale, A.D. (2015), "Effect of high temperature on compressive strength of concrete", *IOSR J. Mech. Civil Eng*., **12**(1), 66-70.
Naaman, A.E. (1985), "Fiber reinforcement for concrete", *ACI Concrete Int*., **7**(3), 21-25.
Ozawa, M. and Morimoto, M. (2014), "Effects of various fibres on high-temperature spalling in high-performance concrete", *Constr. Build. Mater*., **71**, 83-92.
Ozawa, M., Bo, Z., Uchida, Y. and Morimoto, H. (2014), "Preventive Effects of Fibers on Spalling of UFC at High Temperatures", *J. Struct. Fire Eng*., **5**(3), 229-238.
Phan, L.T. and Carino, N.J. (1998), "Review of mechanical properties of HSC at elevated temperature", *J. Mater. Civil Eng*., **10**(1), 58-64.
Phan, L.T. and Carino, N.J. (2002), "Effects of test conditions and mixture proportions on behavior of high-strength concrete exposed to high temperatures", *ACI Mater. J*., **99**(1), 54-66.
Poon, C.S., Shui, Z.H. and Lam, L. (2004), "Compressive behavior of fiber reinforced high performance concrete subjected to elevated temperature", *Cement Concrete Res*., **34**(12), 2215-2222.
Purkiss, J.A. (2007), *Fire safety engineering design of structures*, Butterworth-Heinemann, Elsevier, Oxoford, UK.
Qu, X., Chen, Z., Nethercot, D.A., Gardner, L. and Theofanous, M. (2015), "Push-out tests and bond strength of rectangular CFST columns", *Steel Compos. Struct., Int. J*., **19**(1), 21-41.
Sanjayan, G. and Stocks, L.J. (1993), "Spalling of high-strength silica fume concrete in fire", *ACI Mater. J*., **90**(2), 170-173.
Sideris, K.K., Manita, P. and Chaniotakis, E. (2009), "Performance of thermally damaged fiber reinforced concretes", *Constr. Build. Mater*., **23**(3), 1232-1239.
Siddique, R. and Kaur, D. (2012), "Properties of concrete containing ground granulated blast furnace slag (GGBFS) at elevated temperatures", *J. Adv. Res*., **3**(1), 45-51.
Somayaji, S. (2001), *Civil engineering materials*, Prentice Hall, Upper Siddle River, NJ, USA.
Song, T.Y., Han, L.H. and Yu, H.X. (2010), "Concrete filled steel

tube stub columns under combined temperature and loading", *J. Constr. Steel Res.*, **66**(3), 369-384.
Swamy, R.N. and Mangat, P.S. (1974), "Influence of fiber geometry on the properties of steel fiber reinforced concrete", *Cem. Concr. Res.*, **4**(3), 451-465.
Taiwan Construction and Planning Agency (2004), *Design Code and Commentary for Steel Reinforced Concrete Structures*, Taipei. [In Chinese]
Tao, Z., Ghannama, M., Song, T.Y. and Han, L.H. (2016), "Experimental and numerical investigation of concrete-filled stainless steel columns exposed to fire", *J. Constr. Steel Res.*, **118**, 120-134.
Tatnall, P.C. (2002), "Shortcrete in fires: Effects of fibers on explosive spalling", *Shortcrete*, **4**(4), 10-12.
Toumi, B., Resheidat, M., Guemmadi, Z. and Chabil, H. (2009), "Coupled effect of high temperature and heating time on the residual strength of normal and high-strength concretes", *Jordan J. Civil Eng.*, **3**(4), 322-330.
Wan, C.Y. and Zha, X.X. (2016), "Nonlinear analysis and design of concrete-filled dual steel tubular columns under axial loading", *Steel Compos. Struct., Int. J.*, **20**(3), 571-597.
Xu, M., Hallinan, B. and Wille, K. (2016), "Effect of loading rates on pullout behavior of high strength steel fibers embedded in ultra-high performance concrete", *Cement Concrete Compos.*, **70**, 98-109.
Yan, Z., Shen, Y., Zhu, H., Li, X. and Lu, Y. (2015), "Experimental investigation of reinforced concrete and hybrid fibre reinforced concrete shield tunnel segments subjected to elevated temperature", *Fire Safety J.*, **71**, 86-99.

CC